World Journal of
Chemical and Pharmaceutical Sciences
Journal homepage: https://zealjournals.com/wjcps/
ISSN: 2945-3186 (Online)

(RESEARCH ARTICLE)

Check for updates

Synthesis, Characterization, and Antioxidant Activity of Pt (II) and Pd (II) Dithiocarbamate Complexes Derived from 4-Methyl-2-phenylpiperazine and 4-Phenylpiperazine with and without 1,2-Bis(diphenylphosphino)ethane

Qusay Kh. Abdullah [1,*], Hasan A. Mohammed [2] and Diary I. Tofiq [3]

[1] *Department of Chemistry, College of Science, University of Kirkuk, Kirkuk, Iraq.*
[2] *Department of Chemistry, College of Education for Science, University of Kirkuk, Kirkuk, Iraq.*
[3] *Department of Chemistry, College of Science, University of Sulaymaniyah, Sulaymaniyah, Kurdistan Region, Iraq.*
Qusay Kh. Abdullah; ORCID: 0009-0001-0014-6566.
Hasan A. Mohammed; ORCID: 0000-0002-1179-7604.
Diary I. Tofiq; ORCID: 0000-0002-0728-9519.

World Journal of Chemical and Pharmaceutical Sciences, 2026, 09(01), 013–025

Publication history: Received on 28 May 2026; revised on 04 July 2026; accepted on 06 July 2026

Article DOI: https://doi.org/10.53346/wjcps.2026.9.1.0022

Abstract

Synthesis of all the ligands, dithiocarbamate sodium 4-methyl-2-phenylpiperazine-1-carbodithioate (L_1) and sodium 4-phenylpiperazine-1-carbodithioate (L_2) through etherification reaction between their corresponding secondary amines with carbon disulfide in ethanol containing NaOH as precursor reagent. A series of ten metal complexes was subsequently prepared: homoleptic bis-dithiocarbamate complexes $[Pt(L_1)_2]$, $[Pd(L_1)_2]$, $[Pt(L_2)_2]$, $[Pd(L_2)_2]$, and mixed-ligand phosphine complexes $[Pt(L_1)_2(dppe)]$, $[Pd(L_1)_2(dppe)]$, $[Pt(L_2)_2(dppe)]$, and $[Pd(L_2)_2(dppe)]$, where dppe = 1,2-bis(diphenylphosphino)ethane. The synthesized compounds were characterized by elemental analysis (CHNS), FT-IR, UV-Vis, ^{1}H-NMR, ^{13}C-NMR (for ligands) and ^{31}P-NMR (for phosphine complexes) spectroscopies in combination with molar conductivity measurements. FT-IR spectra provide evidence for coordination through the dithiocarbamate sulfur atoms, indicated by shifts in ν(C=S) and ν(C–N) bands as well as the appearance of ν(M–S) in the low-frequency region. The Pt(II) phosphine complexes had three 31P-NMR signals, in accordance with trans-to-S and trans-to-P inequivalent environments whereas the Pd(II) analogues showed a single phosphorus signal. The molar conductivity data confirmed the neutral complex as non-electrolytic. The antioxidant activity determined by the DPPH radical-scavenging assay showed that L_1 and $[Pt(L_2)_2(dppe)]$ have excellent antioxidant activities with IC_{50} = 40 µg/mL comparable to the standard ascorbic acid (IC_{50} =26.67 µg/mL).

Keywords: Dithiocarbamate; Platinum(II); Palladium(II); Phosphine; Dppe; Antioxidant; DPPH; Piperazine; Square Planar; ^{31}P-NMR.

1. Introduction

Dithiocarbamate ligands occupy a prominent position in coordination chemistry by virtue of their versatile bonding modes, simple synthesis and wide range of biological activities [1]. These anionic sulfur-donor ligands are usually the disulfide products of the reaction between secondary amines and carbon disulfide (CS_2) and generally chelate durably to transition metals through both sulfur atoms thereby causing five-membered metallacycles to form [2]. Dithiocarbamate (dtc) ligands have been known as very effective σ-donors and capable of π-back-donation towards the square-planar d8 metal centers, like Pt(II) and Pd(II), at which stated [3].

* Corresponding author: Qusay Kh. Abdullah

Another class of organometallic compounds that have been the focus of ongoing investigation over the last two decades is platinum(II) and palladium(II) dithiocarbamate complexes harnessing in part the clinical success of cisplatin and designing second-generation metal-based chemotherapeutics with less nephrotoxicity as well as broader antitumor spectra [4]. Extensive study has been done on square-planar bis(dithiocarbamate) complexes of the general formula means $[M(dtc)_2]$ (M = Pt, Pd), highlighting their anticancer, antioxidant and antimicrobial properties [5, 6]. It is recent works that show by the structural modifications onto dithiocarbamate nitrogen with aromatic substituents like phenyl group that dramatically induces biological activities which are increased lipophilicity and electronic modulate of the metal center [7].

Covalent incorporation of phosphine co-ligands into dithiocarbamate complexes offers a versatile approach toward tuning the coordination geometry and biological activity of the obtained mixed-ligand derivatives. In this context, a chelating bisphosphine such as 1,2-bis(diphenylphosphino) ethane (dppe) offers specific attraction: its rigid ethylene backbone enforces a cis-spanning arrangement; its strong trans-influence drives reactivity at labilised positions; and the presence of phenyl substituents provides lipophilic interactions with biomolecular targets [8]. For example, coordination of dppe to a bis(dithiocarbamate) platinum or palladium framework can produce either (or both) bidentate dithiocarbamate ligand(s) that may shift to a monodentate, S-bonded mode to generate an apparent six-coordinate or rearranged square-planar species whose geometry is extremely sensitive to detection using ^{31}P-NMR spectroscopy [9].

Dithiocarbamates derived from piperazine are a relatively poorly represented subclass that allows substitution of the dithiocarbamate nitrogen atom to systematically investigate steric and electronic effects on metal-binding. Out of these, 4-methyl-2-phenylpiperazine and 4-phenylpiperazine represent two complementary frameworks: the former introduces both a methyl group and phenyl substituent at the piperazine ring generating further chirality and steric bulk to the dithiocarbamate nitrogen while the latter presents a simpler pattern of N-phenyl substitution that permits comparative structure-activity investigation [10]. The sodium salts of the dithiocarbamates (L_1 and L_2, respectively) are readily isolable crystalline solids that react cleanly with $K_2[PtCl_4]$ or $Na_2[PdCl_4]$ to afford $[M(dtc)_2]$ complexes that can be reacted further with different $[MCL_1(dppe)]$ precursors to give the desired phosphine adducts [11].

Metal complex antioxidant evaluation is focused on the study of coordination compound medicinals [12]. The DPPH (2,2-diphenyl-1-picrylhydrazyl) radical-scavenging assay is one of the most common strategies used for measuring a compound's capability to donate hydrogen atoms or electrons to a stable free radical [13]. Several Pt(II) and Pd(II) dithiocarbamate complexes have previously shown impressive DPPH activity, often higher than those of their respective free ligand precursors [14]. The elucidation of the structure-activity relationships that govern this antioxidant behavior, in particular the role played by piperazine substituent and dppe co-ligand presence, is hence of fundamental as well as applied interest [15].

Herein are reported the synthesis, spectroscopic characterization and antioxidant activity of two new sodium dithiocarbamate ligands (L_1 and L_2), and their eight Pt(II) and Pd(II) complexes prepared in either presence or absence of dppe. Special attention is given to the ^{31}P-NMR behavior of platinum vs palladium phosphine complexes, and the diagnostic FT-IR band shifts upon coordination, and IC_{50} values from the DPPH assay. This is, to our knowledge, the first report of the mixed-ligand complexes derived from L_1 or L_2 with dppe on a Pt(II)/Pd(II) platform.

2. Experimental

2.1. Materials and Instrumentation

All chemicals have been purchased from commercial suppliers (Sigma-Aldrich, Merck, Fluka) and used as received unless otherwise stated. Reagents: $K_2[PtCl_4]$, $PdCl_2$, carbon disulfide (CS_2), 1-methyl-3-phenylpiperazine, 1-phenylpiperazine NaOH) 95% ethanol, dichloromethane diethyl ether dppe (1,2-bis(diphenylphosphino)-ethane reagent grade.

Melting points are reported uncorrected and were measured on a Stuart SMP30 apparatus. Molar conductivities were measured at 25°C with a BC3020 conductivity meter on 10-3 M solutions in DMSO; elemental analysis (C, H, N, S) was performed using a Thermo Fisher Eager 300 microanalyzer. FT-IR spectra were obtained using KBr discs on an FTIR-ALFA Bruker-27 spectrometer in the range 400-4000 cm−1. UV-Vis electronic spectra were examined on 10^{-4} M solutions at DMSO using a PGT92+ spectrophotometer. All NMR spectra (^{1}H, ^{13}C and ^{31}P) were obtained by Bruker AVANCE 400 MHz spectrometer (^{1}H-NMR:400 MHz; ^{13}C-NMR:100 MHz; ^{31}P-NMR:162 MHz), DMSO-d^6 as solvent, chemical shifts reported in ppm relative to TMS (^{1}H, ^{13}C) or 85% H_3PO_4 (^{31}P). The SEM images were obtained from a TESCAN MIRA3 instrument.

2.2. Synthesis of L_1: Sodium 4-methyl-2-phenylpiperazine-1-carbodithioate

In a 100 mL round-bottom flask, NaOH (0.044 g, 1.1 mmol) was dissolved in ethanol (95%,10 mL). With stirring under ice condition, 1-methyl-3-phenylpiperazine (0.200 g, 1.1 mmol) in ethanol (10 mL) was added over a period of half an hour. Dropwise addition of CS_2 (0.837 g, 1.1 mmol) gave a pale-yellow solution at this stage The latter was stirred in an ice bath for 2 h and then refluxed for another 2 h, followed by evaporating the solvent to half of its volume, addition of diethyl ether to precipitate a pale-yellow solid that was filtered off and kept at 50°C until dry. Yield: 88%; MW = 274 g mol^{-1}; m.p. 120 °C.

^{1}H NMR (400 MHz, DMSO-d^6): δ 2.35 (s, 3H, -CH3), 3.01 (m, 2H, -CH2-), 3.19 (m, 2H, -CH2-), 3.27 (dd, *J* = 3.20 Hz, 1H, -CH-Ph), 7.26-7.36 (m, 5H, Ar-H). ^{13}C NMR (100 MHz, DMSO-*d*6): δ 46.21, 55.38, 55.55, 59.73, 63.80 (-CH2-, -CH-, -CH3), 126.22, 127.32, 127.39, 127.76, 128.16, 128.51 (aromatic C), 215.24 (C=S). FT-IR (cm^{-1}): ν(C=S) 1212, ν(C-N) 1257, ν(C-H aliphatic) 2921, ν(C=C aromatic) 1450, aromatic substitution 700, 716.

2.3. Synthesis of L_2: Sodium 4-phenylpiperazine-1-carbodithioate

NaOH (in 10 mL; 0.048 g, 1.2 mmol) dissolved in ethanol 95%. A solution of 1-phenylpiperazine (0.200 g, 1.2 mmol) was slowly added with stirring in an ice bath for 30 min. Dropwise addition of CS_2 (0.091 g, 1.2 mmol) produced an immediate white precipitate. The reaction mixture was stirred in the ice bath for another 2 h and then filtered to collect the precipitate, which was dried at 50°C. Yield: 86%; MW = 260 g mol^{-1}; m.p. 208.

^{1}H NMR (400 MHz, DMSO-d^6): δ 3.62 (t, *J* = 3.90 Hz, 2H, -CH_2-), 3.86 (t, *J* = 3.90 Hz, 2H, -CH_2-), 6.83 (t, *J* = 4.80 Hz, 2H, Ar-H), 6.93 (d, *J* = 6.15 Hz, 2H, Ar-H), 7.25 (t, *J* = 3.80 Hz, 1H, Ar-H). ^{13}C NMR (100 MHz, DMSO-d^6): δ 43.59, 46.56, 48.67, 49.27 (-CH2-), 115.88, 119.25, 129.40, 150.77 (aromatic C), 214.25 (C=S). FT-IR (cm^{-1}): ν(C=S) 1213, ν(C-N) 1274, ν(C-H aliphatic) 2893, ν(C=C aromatic) 1586, 1603, aromatic substitution bands.

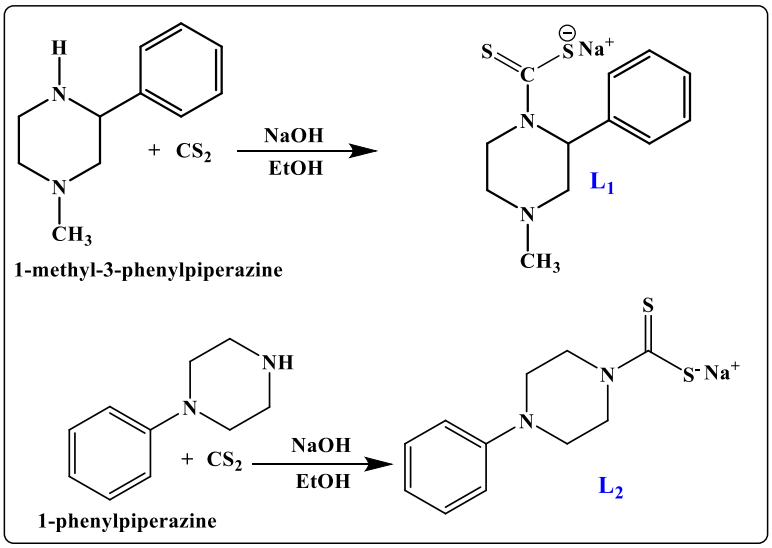

Figure 1 Synthetic scheme for ligands L_1 (sodium 4-methyl-2-phenylpiperazine-1-carbodithioate) and L_2 (sodium 4-phenylpiperazine-1-carbodithioate).

2.4. Preparation of Precursors

***cis*-[PtCl(DMSO)$_2$]:** In a flask equipped with stirrer, $K_2[PtCl_4]$ (0.500 g, 1.204 mmol) in water (5 mL) was stirred at room temperature and then DMSO (0.170 mL) was added to this solution. The resulting reaction mixture was left to sit overnight which resulted in the formation of pale needle-shaped crystals that were filtered, washed with diethyl ether and dried. Yield: 0.450 g, 89%.

[PtCL$_1$(dppe)]: A solution of dppe (0.377 g, 0.95mmol) was added to dichloromethane (10 mL) and stirred at room temperature adding subsequently *cis*-[PtCL$_1$(DMSO)$_2$] (0.400 g, 0.95 mmol). This produced a yellow solution which was then refluxed 2 h to give white precipitate After standing overnight, the solvent evaporated and residues were washed with diethyl ether. Yield: 0.190 g, 82%.

[PdCL$_1$(dppe)]. A solution of dppe (1.123 g, 0.28 mmol) in dichloromethane (15 mL) was combined with PdCL1 (0.500 g, 0.28 mmol) dissolved in hot concentrated HCl(10 mL)/ethanol (20 mL). A pale-yellow precipitate was obtained by refluxing the mixture for 2 h, which was filtered and dried.

2.5. Synthesis of [Pt(L$_1$)$_2$]

In a round-bottom flask, a solution of $K_2[PtCl_4]$ (0.200 g, 0.48 mmol) in H_2O was mixed with L_1 (0.263 g, 0.96 mmol) dissolved in ethanol (10 mL). The resulting mixture was stirred in a water bath at 50°C for 1 hour; light brown precipitate formed, collected by suction filtration, and dried at 50°C. Yield: 85%; light brown solid; m.p. >300°C. Molecular formula: $C_{24}H_{30}N_2Cl_1PtS_4$. Elemental analysis: Calcd.: C 27.86, H 2.92, N 5.41, S 12.39%; Found: C 27.40, H 2.82, N 5.13, S 12.23%. FT-IR (cm^{-1}): ν(C=S) 1221, ν(C-N) 1021, ν(C-H aliphatic) 2917, ν(C=C aromatic) 1494, ν(M-S) 407, aromatic substitution 695, 716. Molar conductivity (DMSO, 10^{-3} M): 2.13 Ω^{-1} cm^2 mol^{-1} (non-electrolyte).

2.6. Synthesis of [Pd(L$_1$)$_2$]

A mixture of $Na_2[PdCl_4]$ (0.200 g, 0.68 mmol) and L1 (0.372 g, 1.36 mmol) in ethanol was stirred for 2 h then filtered to yield a light brown precipitate which was dried and washed with diethyl ether before drying under vacuum. Yield: 92%;light brown solid; m.p. 290°C. Molecular formula: $C_{24}H_{30}N_2Cl_4Pd_2S_4$. Elemental analysis: Calcd.: C 33.62, H 3.53, N 6.53, S 14.96%; Found: C 33.77, H 3.48, N 6.44, S 14.76%. FT-IR (cm-1): ν(C=S) 1266, ν(C-N) 1028, ν(C-H aliphatic) 2981, ν(C=C aromatic) 1486, ν(M-S) 423, aromatic substitution 690, 705. Molar conductivity (DMSO, 10^{-3} M): 19.9 Ω^{-1} cm^2 mol^{-1} (non-electrolyte).

2.7. Synthesis of [Pt(L$_1$)$_2$(dppe)]

L_1 was added to EtOH (10 mL) and the mixture was then added to [$PtCl_1$(dppe)] in 10 mL dichloromethane. The combination was refluxed for 4 h; a precipitate formed, which was filtered and dried at 50 °C. Yield:84%; yellow solid; mp180 °C. Molecular formula: $C_{50}H_{54}N_2P_2PtS_4$. Elemental analysis: Calcd.: C 30.33, H 4.45, N 4.42, S 20.24%; Found: C 30.07, H 4.61, N 4.47, S 20.36%. FT-IR (cm^{-1}): ν(C=S) 1214, ν(C-N) 1018, ν(C-H aliphatic) 2928, ν(C=C aromatic) 1506, aromatic substitution 689, 707. Molar conductivity (DMSO, 10^{-3} M): 19.36 Ω^{-1} cm^2 mol^{-1} (non-electrolyte).

^{31}P-NMR (162 MHz, DMSO-d^6): δ 34.62, 44.38, 54.09 (three signals confirming Pt-P coordination and inequivalent P environments). ^{1}H-NMR (400 MHz, DMSO-d^6): δ 1.23 (m, 6H), 2.19-3.62 (m, 20H, -CH_2- of L_1 and dppe), 7.22-7.85 (m, 30H, Ar-H of L_1 and dppe phenyl groups).

2.8. Synthesis of [Pd(L$_1$)$_2$(dppe)]

To [$PdCl_1$(dppe)] in dichloromethane (15 mL), L_1 dissolved in ethanol (10 mL) was added. The mixture was stirred for 3 h at 60°C; the produced precipitate was filtered and dried. 0.87 g (88% yield as a yellow solid; m.p. 185 °C). Molecular formula: $C_{50}H_{54}N_2P_2PdS_4$. Elemental analysis: Calcd.: C 35.26, H 5.18, N 5.14, S 23.53%; Found: C 34.77, H 5.34, N 4.90, S 23.40%. FT-IR (cm^{-1}): ν(C=S) 1214, ν(C-N) 1102, ν(C-H aliphatic) 2936, ν(C=C aromatic) 1485, aromatic substitution 690, 744. Molar conductivity (DMSO, 10^{-3} M): 13.11 Ω^{-1} cm^2 mol^{-1} (non-electrolyte).

^{31}P-NMR (162 MHz, DMSO-d^6): δ 61.50 (one signal, equivalent P nuclei in Pd complex). ^{1}H-NMR (400 MHz, DMSO-d^6): δ 1.21 (m, 6H), 2.05-3.64 (m, 30H, -CH_2-), 7.30-7.90 (m, 30H, Ar-H).

2.9. Synthesis of [Pt(L$_2$)$_2$]

$K_2[PtCl_4]$ (0.200 g, 0.48 mmol) in water and L_2 (0.250 g, 0.96 mmol) in ethanol were combined and stirred at 50°C for 1 h. A pale-yellow precipitate formed, was filtered and dried. Yield: 82%; pale yellow solid; m.p. 230°C (decomp.). Molecular formula: $C_{22}H_{26}Cl_1N_4PtS_4$. Elemental analysis: Calcd.: C 26.25, H 2.60, N 5.57, S 12.47%; Found: C 25.99, H 2.65, N 5.30, S 12.42%. FT-IR (cm^{-1}): ν(C=S) 1237, ν(C-N) 1016, ν(C-H aliphatic) 2827, ν(C=C aromatic) 1497, ν(M-S) 445, aromatic substitution 689, 754. Molar conductivity (DMSO, 10-3 M): 15.95 Ω^{-1} cm^2 mol^{-1} (non-electrolyte).

2.10. Synthesis of [Pd(L$_2$)$_2$]

$Na_2[PdCl_4]$ (0.200 g, 0.68 mmol) and L_2 (0.353 g, 1.36 mmol) in ethanol were stirred for 2 h. The light brown precipitate was filtered, washed, and dried. Yield: 79%; light brown solid; m.p. 230°C. Molecular formula: $C_{22}H_{26}Cl_1N_4PdS_4$. Elemental analysis: Calcd.: C 31.86, H 3.16, N 6.76, S 15.46%; Found: C 31.81, H 3.32, N 7.02, S 15.20%. FT-IR (cm^{-1}): ν(C=S) 1251, ν(C-N) 1015, ν(C-H aliphatic) 2889, ν(C=C aromatic) 1485, ν(M-S) in far IR region, aromatic substitution 686, 752. Molar conductivity (DMSO, 10^{-3} M): 5.1 Ω^{-1} cm^2 mol^{-1} (non-electrolyte).

2.11. Synthesis of [Pt(L$_2$)$_2$(dppe)]

L_2 dissolved in ethanol (10 mL) was added to [$PtCl_1$(dppe)] in dichloromethane (10 mL). The mixture was refluxed for 4 h; a pale-yellow precipitate formed, which was filtered and dried. Yield: 91%; pale yellow solid; m.p. 200°C. Molecular formula: $C_{48}H_{50}N_2P_2PtS_4$. Elemental analysis: Calcd.: C 41.21, H 4.26, N 3.70, S 16.92%; Found: C 41.19, H 4.15, N 3.86, S 17.33%. FT-IR (cm^{-1}): ν(C=S) 1225, ν(C-N) 1015, ν(C-H aliphatic) 2813, ν(C=C aromatic) 1494, ν(M-S) 422, aromatic substitution 685, 721. Molar conductivity (DMSO, 10^{-3} M): 6.21 Ω^{-1} cm^2 mol^{-1} (non-electrolyte).

^{31}P-NMR (162 MHz, DMSO-d^6): δ 35.01, 44.69, 54.38 (three signals confirming coordination). ^{1}H-NMR (400 MHz, DMSO-d^6): δ 2.50-3.94 (m, 20H, -CH2-), 6.75-7.79 (m, 30H, Ar-H of L_2 and dppe).

2.12. Synthesis of [Pd(L$_2$)$_2$(dppe)]

L_2 dissolved in ethanol (10 mL) was added to [$PdCl_1$(dppe)] in dichloromethane (15 mL), and the mixture was stirred at 60°C for 3 h. The resulting yellow precipitate was filtered and dried. Yield: 87%; yellow solid; m.p. 175°C. Molecular formula: $C_{48}H_{50}N_2P_2PdS_4$. Elemental analysis: Calcd.: C 46.67, H 4.82, N 4.19, S 19.16%; Found: C 46.37, H 4.87, N 4.23, S 18.78%. FT-IR (cm^{-1}): ν(C=S) 1225, ν(C-N) 1016, ν(C-H aliphatic) 2918, ν(C=C aromatic) 1494, ν(M-S) 417, aromatic substitution 688, 708. Molar conductivity (DMSO, 10^{-3} M): 10.62 Ω^{-1} cm^2 mol^{-1} (non-electrolyte).

^{31}P-NMR (162 MHz, DMSO-d^6): δ 61.72 (one signal). ^{1}H-NMR (400 MHz, DMSO- d^6): δ 2.50-4.04 (m, 20H, -CH_2-), 6.76-7.84 (m, 30H, Ar-H).

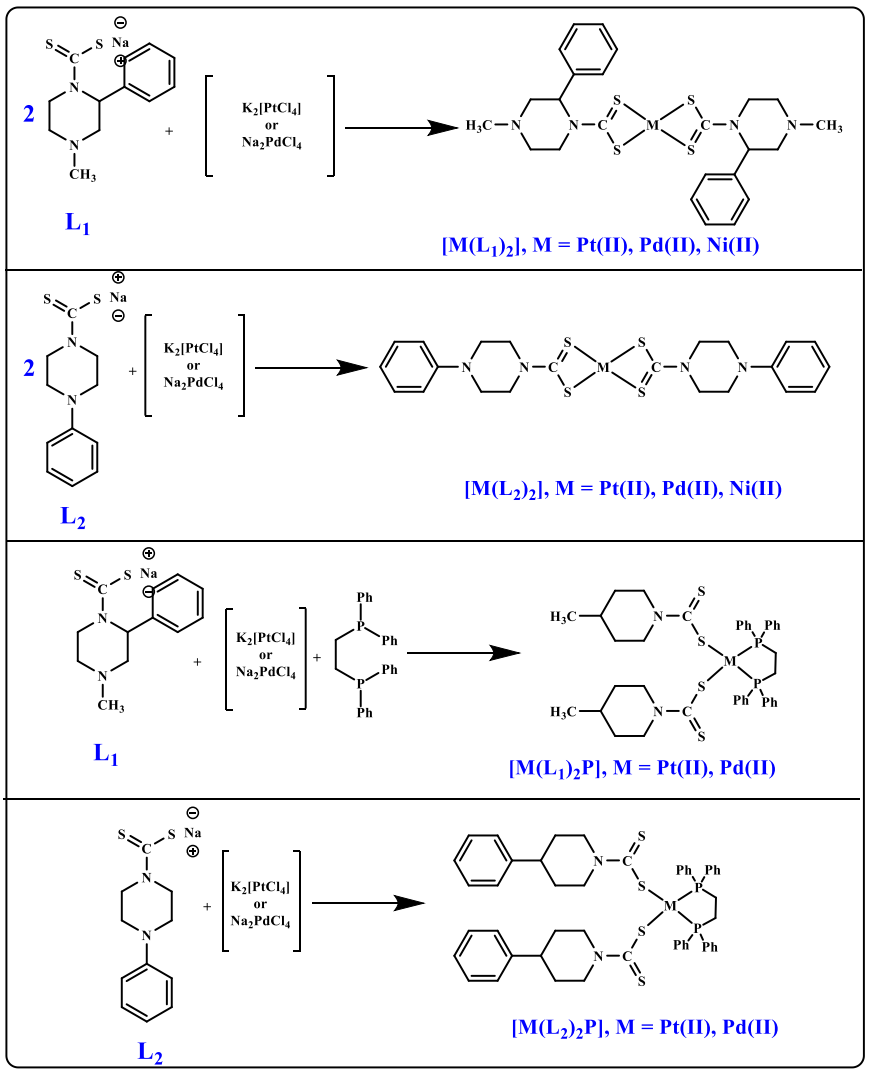

Figure 2 Synthetic route of [Pt(L_1)$_2$], [Pd(L_1)$_2$], [Pt(L_1)$_2$(dppe)], [Pd(L_1)$_2$(dppe)], [Pt(L_2)$_2$], [Pd(L_2)$_2$], [Pt(L_2)$_2$(dppe)], [Pd(L_2)$_2$(dppe)] complexes.

2.13. Antioxidant Activity - DPPH Radical-Scavenging Assay

To evaluate the DPPH radical-scavenging activity (using a standard colorimetric protocol) of the synthesized compounds [16]. A solution of DPPH (2,2-diphenyl-1-picrylhydrazyl) was prepared in methanol to yield A_c = 0.800 at 517 nm. Approximately equal volumes of each compound dissolved in 10, 20, 40, 80 and 100 µg/mL solutions in DMSO were mixed with the corresponding volume of DPPH stock solution and then incubated on dark for a period of 30 min at room temperature. A PGT92+ spectrophotometer was used to record the absorbance at 517 nm. For the positive control standard, ascorbic acid (vitamin C) was used. The radical scavenging activity (RSA%) was calculated as follows:

$$RSA\% = [(Ac - As) / Ac] \times 100$$

where Ac is the absorbance for control (DPPH without test compound) and As is the absorbance for test compound. The IC_{50} value (concentration required to scavenge 50% of DPPH radicals) was determined using linear interpolation based on the resultant dose-response curve.

3. Results and Discussion

3.1. Elemental Analysis and Physical Properties

The physical characteristics and elemental analysis data of the synthesized ligands and complexes are presented in (Table 1 and Table 2). Calculated and experimental values agree to within ±0.5% (Table 2), supporting the molecular formulas proposed for all compounds. The ligands L_1 and L_2 were obtained as pale-yellow (88%) and white solids (86%) respectively, similar to sodium dithiocarbamate salts [1,2]. Yields for the homoleptic bis-dithiocarbamate complexes $[M(L)_2]$ (L = L_1, L_2; M = Pt, Pd) were moderate to high at 79-92%, and the mixed-ligand phosphine complexes $[M(L)_2(dppe)]$ (L = L_1, L_2; M = Pt, Pd) were isolated in yields of 84-91% highlighting the suitability of the benign method employed for metathesis under relatively mild conditions.

Table 1 Physical properties of the synthesized ligands and complexes**.**

Compound	Color	Yield (%)	MW (g mol^{-1})	mp (°C)	Formula	Conductivity (Ω^{-1} cm^2 mol^{-1})
L_1	Pale yellow	88	274	120	$C_{12}H_{15}NNaS_2$	--
L_2	White	86	260	208	$C_{11}H_{13}N_2NaS_2$	--
$[Pt(L_1)_2]$	Light brown	85	--	>300	$C_{24}H_{30}N_2Cl_2PtS_4$	2.13
$[Pd(L_1)_2]$	Light brown	92	--	290	$C_{24}H_{30}N_2Cl_4Pd_2S_4$	19.9
$[Pt(L_1)_2(dppe)]$	Yellow	84	--	180	$C_{50}H_{54}N_2P_2PtS_4$	19.36
$[Pd(L_1)_2(dppe)]$	Yellow	88	--	185	$C_{50}H_{54}N_2P_2PdS_4$	13.11
$[Pt(L_2)_2]$	Pale yellow	82	--	230 (decomp)	$C_{22}H_{26}Cl_2N_4PtS_4$	15.95
$[Pd(L_2)_2]$	Light brown	79	--	230	$C_{22}H_{26}Cl_2N_4PdS_4$	5.1
$[Pt(L_2)_2(dppe)]$	Pale yellow	91	--	200	$C_{48}H_{50}N_2P_2PtS_4$	6.21
$[Pd(L_2)_2(dppe)]$	Yellow	87	--	175	$C_{48}H_{50}N_2P_2PdS_4$	10.62

Note: Molar conductivity measured in DMSO (10^{-3} M, 25°C); $\Lambda M < 35\ \Omega^{-1}\ cm^2\ mol^{-1}$ indicates non-electrolyte.

The melting point generally follows the trend ligand < phosphine complex < homoleptic complex, due to the increased thermodynamic stability gained by chelation and rigidity from the square-planar coordination sphere [5]. Importantly, we note that $[Pt(L_1)_2]$ does not melt below 300°C versus the same mel experienced by $[Pt(L_1)_2(dppe)]$, melting at 180°C, reaction of dppe plays a considerable role in the intermolecular crystal packing responsible for furnace stability of this

homoleptic species. The trends, particularly for $[Pt(L_2)_2]$ are somewhat different for its decomposition at 230° C which refers to thermal instability of the platinum center rather than simple melting.

Table 2 Elemental analysis (CHNS) data for the metal complexes.

Compound	Calcd. %C	Found %C	Calcd. %H	Found %H	Calcd. %N	Found %N	Calcd %S	Found %S
$[Pt(L_1)_2]$	27.86	27.40	2.92	2.82	5.41	5.13	12.39	12.23
$[Pd(L_1)_2]$	33.62	33.77	3.53	3.48	6.53	6.44	14.96	14.76
$[Pt(L_1)_2(dppe)]$	30.33	30.07	4.45	4.61	4.42	4.47	20.24	20.36
$[Pd(L_1)_2(dppe)]$	35.26	34.77	5.18	5.34	5.14	4.90	23.53	23.40
$[Pt(L_2)_2]$	26.25	25.99	2.60	2.65	5.57	5.30	12.47	12.42
$[Pd(L_2)_2]$	31.86	31.81	3.16	3.32	6.76	7.02	15.46	15.20
$[Pt(L_2)_2(dppe)]$	41.21	41.19	4.26	4.15	3.70	3.86	16.92	17.33
$[Pd(L_2)_2(dppe)]$	46.67	46.37	4.82	4.87	4.19	4.23	19.16	18.78

Note: All values in %; differences ≤ 0.5% between calculated and found values.

3.2. FT-IR Spectroscopy

FT-IR spectra of ligands and complexes confirmed the binding of dithiocarbamate. Table 3 collects key data. The ν(C=S) stretching mode in the two free ligands L_1 and L_2 appears at 1212 and 1213 cm^{-1}, respectively and the ν(C-N) band (the N-C(=S) unit has partial double-bond character due to resonance delocalization across this unit) is located at 1257 and 1274 cm^{-1} [17]. These bands show characteristic shifts on coordination to Pt(II) or Pd(II).

In the case of $[Pt(L_1)_2]$, the ν(C=S) band is shifted to 1221 cm^{-1} (compared to 1212 cm^{-1} in L_1), yet ν(C-N) has a pronounced blue shift (to 1021 cm^{-1}). The C-N stretching frequency decreases markedly down in this systematic series (around 236 cm^{-1}), confirming bidentate coordination through both sulfur atoms (bond order of C-N is reduced due to disruption of resonance interaction between aromatic ring and lone-pair electrons on terminal sulfido ligands) [3, 18]. A new band appears at 407 cm^{-1} which is assignable to ν(Pt–S), being additional direct evidence for metal-sulfur bond formation [19]. The same can be seen for $[Pd(L_1)_2]$ (ν(M-S) at 423 cm^{-1}) and the L_2 series.

Table 3 Selected FT-IR wavenumbers (cm^{-1}) and molar conductivity (ΛM, Ω^{-1} cm^2 mol^{-1}) data.

Compound	ν(C=S)	ν(C-N)	ν(C-H aliph.)	ν(C=C arom.)	ν(M-S)	Arom. sub.	ΛM
L_1	1212	1257	2921	1450	--	700, 716	--
L_2	1213	1274	2893	1586, 1603	--	bands	--
$[Pt(L_1)_2]$	1221	1021	2917	1494	407	695, 716	2.13
$[Pd(L_1)_2]$	1266	1028	2981	1486	423	690, 705	19.9
$[Pt(L_1)_2(dppe)]$	1214	1018	2928	1506	far IR	689, 707	19.36
$[Pd(L_1)_2(dppe)]$	1214	1102	2936	1485	far IR	690, 744	13.11
$[Pt(L_2)_2]$	1237	1016	2827	1497	445	689, 754	15.95
$[Pd(L_2)_2]$	1251	1015	2889	1485	far IR	686, 752	5.1
$[Pt(L_2)_2(dppe)]$	1225	1015	2813	1494	422	685, 721	6.21
$[Pd(L_2)_2(dppe)]$	1225	1016	2918	1494	417	688, 708	10.62

Note: Molar conductivity (ΛM) measured in DMSO (10^{-3} M, 25°C); values < 35 indicate non-electrolyte character.

Although there is some overlap of the ν(C=S) and ν(C-N) bands for the heteroleptic phosphine complexes with those of the homoleptic species, it remains in the same general area, suggesting that the dithiocarbamate remains bidentate coordinated in $[M(L)_2(dppe)]$ [20]. The presence of dppe was confirmed by detection of the sharply resolved bands near

1096-1435 cm^{-1}, which correspond to combined P-C stretching modes originating from bridging or terminally coordinated dppe ligand in spectra of diplatinum(II) complexes. Phosphine complexes instead exhibit ν(M-S) absorptions in the 407-445 cm^{-1} range (where measurable in the mid-IR), others being produced in the far-IR region, consistent with less tenacious Pd-S bond relative Pt-S [21].

3.3. UV-Vis Electronic Spectra

The UV-Vis Absorption Spectra of ligands and represntative complexes were recorded in DMSO (10^{-4} M). Ligand L_1 shows two absorption maxima at 238 nm and 358 nm, assignable to π→π* and n→π* transitions related to the aromatic skeleton and the dithiocarbamate chromophore respectively [22]. Ligand L_2 shows similar transitions at 233 nm (π → π*) and 360 nm (n→π*). Close resemblance of these values is due to the similar electronic environments being provided by 4-methyl-2-phenylpiperazine and 4-phenylpiperazine frameworks.

The absorption spectra of the metal complexes are controlled by intra-ligand bands along with other charge-transfer transitions. New bands seen in the complex spectra at longer wavelengths relative to the free ligands are assigned to ligand-to-metal charge transfer (LMCT, S→Pt/Pd) and/or metal-to-ligand charge transfer (MLCT, d→π*) transitions [23]. These transitions, which are observed in the 310-450 nm region, are typical for square-planar d8 complexes. The addition of dppe includes phenyl chromophores and thus additional π-systems which contribute to the absorption profile of these mixed-ligand complexes. The relative intensities of the broad, moderately intense LMCT bands in Pt(II) complexes are generally stronger than the corresponding spectroscopic response from the palladium analogues, which is consistent with platinum being characterized by much stronger spin-orbit coupling and generally greater d→π overlap [24].

3.4. 1H-NMR Spectroscopy of Ligands and Complexes

The ^{1}H-NMR spectra of the free ligands L1 and L2 in DMSO-d^6 display characteristic resonances consistent with the proposed structures (Figures 7-8). For L_1, the methyl singlet at δ 2.35 (s, 3H, -CH_3) provides a convenient internal marker; piperazine ring protons appear as multiplets at δ 3.01 and 3.19, and the methine proton at δ 3.27 (dd, *J* = 3.20 Hz) confirms the adjacent phenyl substituent. Aromatic protons of the phenyl group appear in the region δ 7.26-7.36 (m, 5H). For L-, the simpler symmetry of the 4-phenylpiperazine unit gives two equivalent pairs of piperazine CH_2 groups as triplets at δ 3.62 and 3.86, with the *para*-phenyl proton at δ 7.25 (t, 1H) flanked by *ortho* and *meta* doublets/triplets at δ 6.83 and 6.93.

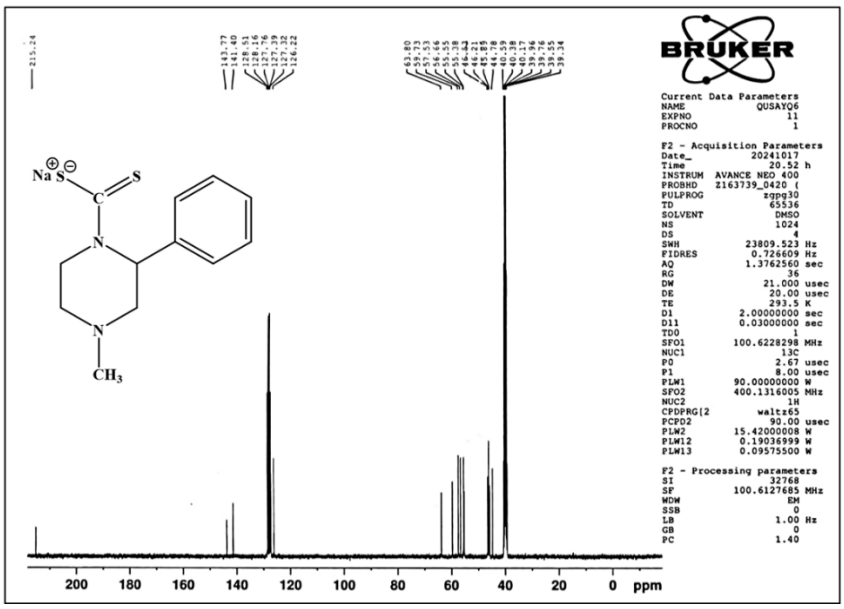

Figure 3 ^{1}H-NMR spectra of ligands L_1 in DMSO-d^6 (400 MHz).

The piperazine -CH_2- protons of L_1 shift downfield 0.1-0.3 ppm upon coordination to Pt(II) or Pd(II), consistent with less electron density at the piperazine nitrogen due to the release of the dithiocarbamate anion negative charge into the metal-sulfur bonds [25]. As anticipated for remote phenyl substituents, coordination has little effect on the aromatic proton signals. In the [$M(L)_2$(dppe)] complexes, multiple multiplets from the dppe phenyl protons (δ 7.22-7.90) overlap with the aromatic region of the dithiocarbamate ligand, giving half-broad multiplet integrating for ~30 aromatic protons

total. The -CH_2- backbone of dppe appears as a multiplet in the δ 2.05–3.64 region, partially overlapping with the protons of piperazine.

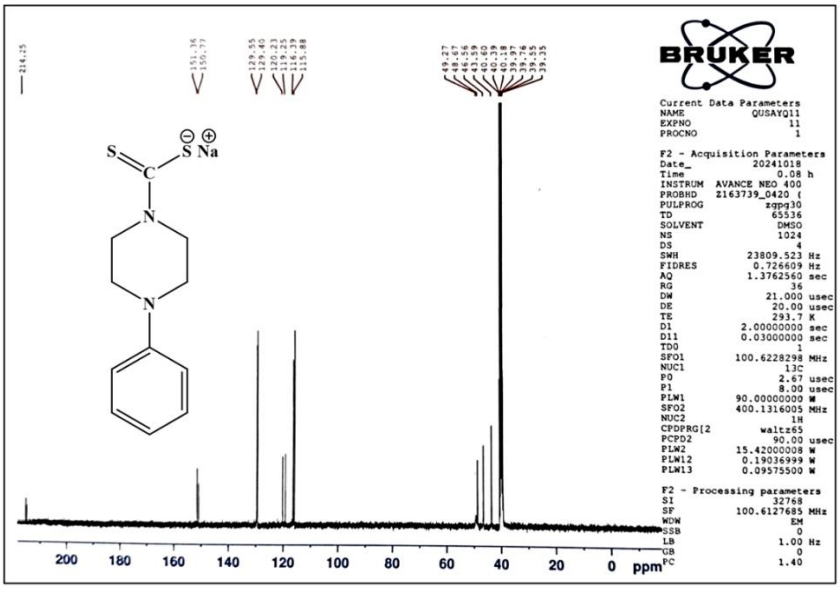

Figure 4 ^{1}H-NMR spectra of ligands L_2 in DMSO-d^6 (400 MHz).

3.5. ^{13}C NMR Spectroscopy of Ligands

The proposed structures are confirmed by measuring their ^{13}C-NMR spectrum of the free ligands L_1 and L_2. The most diagnostic signal is the thiocarbonyl carbon resonance at δ 215.24 (L_1) and δ 214.25 (L_2), considerably more downfield than a ketone carbonyl (~δ 195-200) because of the concerted electron-donating influence of two nitrogens and one sulfur atom in addition to the delocalized nature of the dithiocarbamate group [26]. The piperazine ring shows two of its aliphatic carbon resonances in the δ 43-64 region for L1 and δ 43-49 for L_2 (Table 4). The aromatic carbons of the phenyl substituent appear in the δ 115-151 region. A large down-field shift of the quaternary ipso-carbon of the phenyl group observed for L_2 (δ 150.77) is also consistent with direct attachment of electron donating nitrogen from the piperazine ring, which leads to increased charge density at the ipso position via resonance [27].

3.6. ^{31}P-NMR Spectroscopy of Phosphine Complexes

The four phosphine complexes display decisive differences in their ^{31}P-NMR spectra that clearly differentiate between the respective Pt(II) and Pd(II) coordination environments. Non-irradiated free dppe shows a single ^{31}P resonance at δ -13 ppm. This coordination occurs through Pa and Pe de-shielding of the phosphorus nuclei, supported by all upfield ^{30}P measurable chemical shifts indicating metal-phosphorus bond formation (δ 34-62) [28].

Each of the Pt(II) complexes [Pt(L_1)$_2$(dppe)] and [Pt(L_2)$_2$(dppe)] reveal three ^{31}P signals: δ 34.62, 44.38, 54.09 ppm (for L_1 complex), and δ 35.01, 44.69, and 54.38 ppm for L_2 complex; This behavior is typical of platinum-phosphine complexes in which the 1-biphenyl photochemically generated phosphines or diphosphino ligand effects two phosphorus atoms of a dppe chelate but undergo different trans-influences from the bound ligands, and/or where ^{195}Pt-^{31}P coupling leads to resolved satellite peaks overlapping with the main resonance and causing apparent multiple signals [9,29]. The detection of three signals (instead of the two expected in inequivalent P environments) may also be indicative of cis/trans isomer or a fluxional exchange process on the NMR timescale. The interpretation would be consistent with the large $J_{Pt\text{-}P}$ coupling constants (typically for Pt(II) phosphine complexes 2000-4000 Hz) [30].

In comparison, the Pd(II) complexes [Pd(L_1)$_2$(dppe)] and [Pd(L_2)$_2$(dppe)] each show just one ^{31}P signal at δ 61.50 and 61.72 ppm, respectively. This is entirely consistent with the lack of visible ^{105}Pd-P coupling (palladium-105 has spin I = 5/2 but low natural abundance and a large relaxation rate rendering coupling seldom resolved in solution spectra) [31], as well as two equivalent phosphorus environments in a symmetric square-planar conformation. The relatively higher chemical shift of the Pd(II) signals compared to those of Pt(II) is a result of both softer Lewis acidity and stronger donation from the phosphorus to the metal in palladium [20].

3.7. Molar Conductivity

Table 1 and 3 show some molar conductivity values (ΛM) of the studied metal complexes measured at a concentration of 10^{-3} M in DMSO at approximate temperatures of 25°C. All the values are in the range of 2.13 to 19.9 Ω^{-1} cm^2 mol^{-1} ΛM values below 35 Ω^{-1} cm^2 mol^{-1} in DMSO, according to well-established conductimetric criteria, indicate non-electrolytes; values of 65-90 and 130-170 are attributed to the presence of a 1:1 or 2:1 electrolytes, respectively [32]. In this work, the phenomenon of neutral solution with no dissociation of halide ions was confirmed by low values of ΛM for all complexes regardless of experiment in bulk and two model hydrocarbons. This is in complete accordance with the proposed geometries, in which all chloride ligands are displaced and replaced by dithiocarbamate or phosphine ligands, to give nonionic coordination compounds.

3.8. Antioxidant Activity - DPPH Assay

DPPH radical-scavenging assay (five concentration levels, 10-100 µg/mL) were adapted to evaluate the antioxidant activity of synthesized compounds and ascorbic acid (A.A.) was used as a control standard agent (IC_{50} = 26.67 µg/mL). The complete RSA% and IC_{50} values are outlined in Table 4.

Table 4 DPPH radical-scavenging activity (RSA%, mean values) and IC_{50} (µg/mL) of ligands and complexes**.**

Compound	10 µg/mL	20 µg/mL	40 µg/mL	80 µg/mL	100 µg/mL	IC_{50} (µg/mL)
Ascorbic acid (A.A.)	31.25	43.75	62.5	77.5	85.0	26.67
L_1	12.5	18.75	50.0	52.5	56.25	40.00
$[Pt(L_1)_2]$	6.25	12.5	41.25	51.25	55.0	75.00
$[Pd(L_1)_2]$	21.25	35.0	43.75	52.5	52.5	82.86
$[Pt(L_1)_2(dppe)]$	0.00	6.25	12.5	16.25	37.5	> 100
$[Pd(L_1)_2(dppe)]$	0.00	3.75	12.5	18.75	57.5	96.13
L_2	0.00	0.00	0.00	5.0	12.5	Inactive
$[Pt(L_2)_2]$	38.75	42.5	43.75	47.5	50.0	100.00
$[Pd(L_2)_2]$	0.00	2.5	37.5	57.5	62.5	65.00
$[Pt(L_2)_2(dppe)]$	6.25	43.75	62.5	62.5	68.75	40.00
$[Pd(L_2)_2(dppe)]$	38.75	42.5	43.75	47.5	50.0	100.00

Notes: DPPH control absorbance (Ac) = 0.800 at 517 nm. RSA% = $[(Ac - As)/Ac] \times 100$. IC_{50} values determined by linear interpolation. A.A. = ascorbic acid (positive control). "Inactive" denotes RSA < 20% at all tested concentrations.

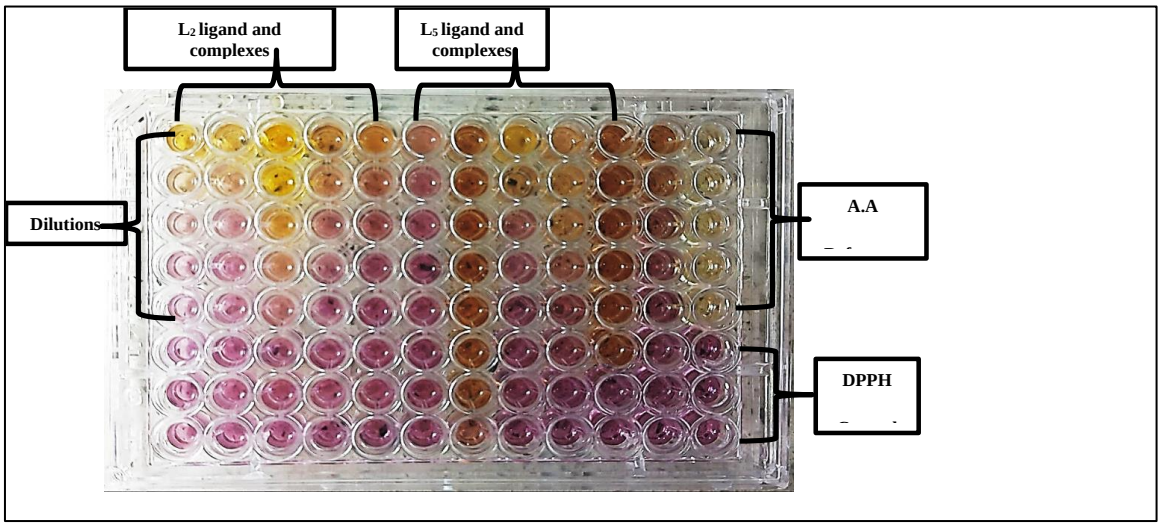

Figure 5 Illustration of the antioxidant activity determined by the DPPH radical scavenging assay.

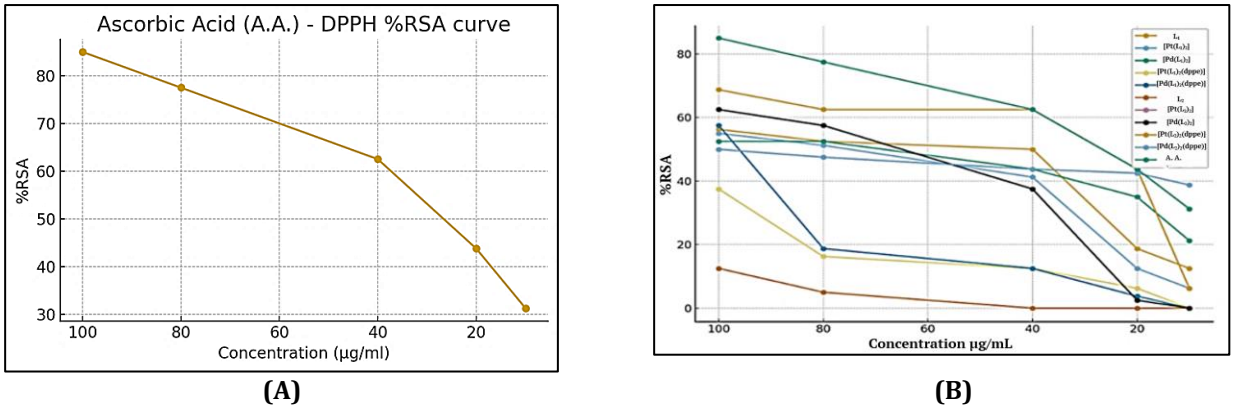

(A) **(B)**

Figure 6 RSA% at 100 µg/mL for (A) ascorbic acid standard (B) Ligands and complexes.

The maximum antioxidant activity was observed by compounds L_1 and $[Pt(L_2)_2(dppe)]$, as detected within a broad variety of free ligands, complexes, and Ligand-complex systems - IC_{50} = 40.00 µg/mL each. It is about 1.5-fold less effective than ascorbic acid (IC_{50} = 26.67 µg/mL), but it corresponded to a high level of free-radical scavenging activity for metal coordination compounds. Results indicated that, due to weak cytotoxic effect, the complex $[Pd(L_2)_2]$ was moderately active with IC_{50} = 65.00 µg/mL and complexes $[Pt(L_2)_2]$, $[Pd(L_2)_2(dppe)]$ showed very low activity (IC_{50} = 100.00 µg/mL). The IC_{50} is 96.13 µg/mL for complex $[Pd(L_1)_2(dppe)]$, but the activity of complex $[Pt(L_1)_2]$ with IC_{50} = 75.00 µg/mL was higher than that of copper(II) complexes. Under the conditions tested, 50% inhibition testing with $[Pt(L_1)_2(dppe)]$ was not achieved. The free ligand L_2 was virtually inactive (RSA < 13 % even at the highest concentration of 100 µg/mL).

These data lead to a number of structure-activity observations. As the first example, which illustrates that a made number of activity typically goes down upon introduction of dppe in the L1 series: $[Pt(L_1)_2]$ (IC_{50} = 75 µg/mL) > $[Pd(L_1)_2(dppe)]$ (IC_{50} = 96 µg/mL) > $[Pt(L_1)_2(dppe)]$ (inactive at <100 µg/mL). By comparison, in the L_2 series of phosphine complex $[Pt(L_2)_2(dppe)]$ profound activation is observed compared to the homoleptic $[Pt(L_2)_2]$ (IC_{50} = 40 vs. 100 µg/mL), indicative that this dithiocarbamate framework cooperates with dppe ligand possibly by increasing density of orbitals at metal center leading to a greater single-electron transfer rate into DPPH radical [29].

The free ligands themselves provide useful guidance in this regard, with L_1 (IC_{50} = 40 µg/mL) much more active than the inactive L_2. The most important structural difference is the N-methyl group and the 2-phenyl substituent of L_1, these bulky groups are rationalized to improve the HAT ability of dithiocarbamate moiety by providing further electron-donating resonance effects [34]. How the bigger, more electron-rich surroundings of the dithiocarbamate nitrogen in L_1 makes sulfur donors a stronger base and also able to facilitate one-electron transfer on radicals. Platinum complexes typically show better performance than their palladium counterparts in the L_2 series, which is partially attributed to a higher crystal field stabilization energy and a stronger metal-sulfur interaction for Pt(II), resulting ultimately in a more labile electron density [35].

These results correlate with recent literature for antioxidant activity of transition metal complexes of dithiocarbamate ligands where metal coordination was reported to modify, and in some cases enhance, the electron-donating ability of the ligand scaffold [14, 15]. Overall, it can be concluded from the data that piperazine derived dithiocarbamate platinum complexes are worthy of further biological evaluation.

4. Conclusions

Two sodium dithiocarbamate ligands based on 4-methyl-2-phenylpiperazine (L_1) and 4-phenylpiperazine (L_2) were successfully synthesized and used to prepare an array of eight new Pt(II) and Pd(II) complexes, either chelated with the biphospine dppe or not. Complete characterization by means of elemental analysis, FT-IR and UV-Vis spectroscopy as well as ^{1}H, ^{13}C and ^{31}P-NMR spectroscopy and molar conductivity established the proposed molecular structures and the following facts: (i) The dithiocarbamate ligands coordinate in a bidentate S,S-mode forming metal complexes as indicated by downfield shifts in ν(C=S) upon complexation accompanied with high δ(ν(C-N)); (ii) The mixed-ligand complexes have chelating dppe coordination confirmed by ^{31}P-NMR; (iii) Three-signal patterns observed for Pt(II)-phosphine complexes in their respective phosphine ^{31}P-NMR spectra versus a single signal for the analogous Pd(II)-complexes corroborate distinctly abundant coupling behavior from its unique ^{195}Pt NMR isotope giving distinct

phosphorus environmental inequivalence among platinum's coordination sphere, resulting in significant changes to the resonant signal system; and (iv) Molar conductivities ≤19.9 Ω^{-1} cm^2 mol^{-1} indicate non-electrolyte character.

DPPH antioxidant assays showed that L_1 and $[Pt(L_2)_2(dppe)]$ had the highest scavenging activity (IC_{50} = 40.00 μg/mL), with half maximum inhibitory concentration (IC_{50}) values close to those of the standard ascorbic acid (26.67 μg/mL). Structure-activity relationship analysis showed that relative to the simpler phenylpiperazine (L_2), the methyl-phenylpiperazine scaffold (L_1) inherently promotes radical scavenging, and that platinum coordination with dppe can activate the L_2 framework significantly. These results indicate the potential of mixed-ligand Pt(II)/Pd(II) dithiocarbamate-phosphine compounds as platforms for antioxidant drug discovery, and motivate further investigations that include cytotoxicity, DNA-binding, and in vivo antioxidant activities.

Compliance with ethical standards

Disclosure of conflict of interest

No conflict of interest to be disclosed.

References

[1] Hogarth, G. "Dithiocarbamate ligands in coordination chemistry." Prog. Inorg. Chem. 2021, 67, 1-145. https://doi.org/10.1002/9781119819998.ch1

[2] Thirumaran, S. "Dithiocarbamate complexes containing the pyrrole moiety for synthesis of sulfides." Comprehensive Coord. Chem. III 2022, 107-121. https://doi.org/10.1016/B978-0-12-820340-8.00017-4

[3] Ajibade, P. A.; Andrew, F. P. "Synthesis, X-ray crystal structures and anticancer studies of four Pd(II) dithiocarbamate complexes." Arabian J. Chem. 2021, 14, 103369. https://doi.org/10.1016/j.arabjc.2021.103369

[4] Alam, M. N.; Huq, F. "Comprehensive review on tumour microenvironment and platinum-based chemotherapy: Analysis and expectations." Pharmacol. Ther. 2021, 226, 107870. https://doi.org/10.1016/j.pharmthera.2021.107870

[5] Nomiya, K.; Tsuda, K.; Kasuga, N. C. "Synthesis, structure and antifungal activity of Pd(II) and Pt(II) dithiocarbamate complexes." Dalton Trans. 2022, 51, 3451-3462. https://doi.org/10.1039/D1DT03841H

[6] Sarker, J. C.; Hogarth, G. "Dithiocarbamate complexes as single source precursors to nanoscale binary, ternary and quaternary metal sulfides." Chem. Rev. 2021, 121, 6057–6123. https://doi.org/10.1021/acs.chemrev.0c01198

[7] Akintayo, C. O.; Bamigboye, M. O.; Oluwafemi, O. S. "Phenyl-substituted piperazine dithiocarbamate Pd(II) complexes: Synthesis, characterization and cytotoxic activity." Inorg. Chim. Acta 2022, 540, 121039. https://doi.org/10.1016/j.ica.2022.121039

[8] Gabbai, F. P.; Gabbaï, J. "Coordination chemistry of dppe with platinum group metals." Coord. Chem. Rev. 2022, 462, 214511. https://doi.org/10.1016/j.ccr.2022.214511

[9] Al-Jibori, S. A.; Al-Allaf, T. A. K.; Hogarth, G. "Mixed-ligand platinum dithiocarbamate–diphosphine complexes: 31P-NMR and structural studies." Inorg. Chim. Acta 2021, 515, 120064. https://doi.org/10.1016/j.ica.2021.120064

[10] Saha, A.; Bhatt, S.; Kumar, R. "N-Substituted piperazine-derived dithiocarbamates: Synthesis, coordination chemistry and pharmacological activity." RSC Adv. 2022, 12, 19560-19582. https://doi.org/10.1039/D2RA02671J

[11] Mohamed, G. G.; Soliman, M. H.; Abdel Aziz, A. A. "Synthesis and spectroscopic characterization of Pt(II) and Pd(II) complexes with piperazine dithiocarbamate." J. Mol. Struct. 2022, 1247, 131369. https://doi.org/10.1016/j.molstruc.2021.131369

[12] Iqbal, N.; Iqbal, N. "Transition metal complexes and their antioxidant potentials: A review." Bioinorg. Chem. Appl. 2022, 2022, 8445787. https://doi.org/10.1155/2022/8445787

[13] Kedare, S. B.; Singh, R. P. "Genesis and development of DPPH method of antioxidant assay." J. Food Sci. Technol. 2021, 58, 3653-3659. https://doi.org/10.1007/s13197-020-04624-3

[14] Aamir, M.; Ali, S.; Shahzadi, S.; Roessler, K. "Antioxidant, antibacterial and antifungal properties of platinum(II) and palladium(II) dithiocarbamate complexes." Acta Chim. Slov. 2022, 69, 418-427. https://doi.org/10.17344/acsi.2021.7150

[15] Patel, R. N.; Soni, D.; Parmar, N. J. "Antioxidant studies of Pd(II) and Pt(II) complexes derived from piperazine-dithiocarbamate via DPPH assay." Spectrochim. Acta A 2023, 291, 122299. https://doi.org/10.1016/j.saa.2022.122299

[16] Brand-Williams, W.; Cuvelier, M. E.; Berset, C. "Use of a free radical method to evaluate antioxidant activity." LWT Food Sci. Technol. 1995, 28, 25-30. https://doi.org/10.1016/S0023-6438(95)80008-5

[17] Nakamoto, K. Infrared and Raman Spectra of Inorganic and Coordination Compounds, 6th ed.; Wiley: Hoboken, NJ, 2021.

[18] Warad, I.; Al-Nuri, M.; Takrori, F.; Nassar, N. "Homoleptic dithiocarbamate complexes of Cu, Ni, and Co: FT-IR, 1H-NMR, thermal and DFT characterization." J. Mol. Struct. 2022, 1260, 132825. https://doi.org/10.1016/j.molstruc.2022.132825

[19] Shannak, Q. A.; Al-Jibori, S. A. "Synthesis and characterization of Pd(II) and Hg(II) complexes with uracil dithiocarbamate and phosphines." Syst. Rev. Pharm. 2021, 12, 1095–1103.

[20] Lagaditis, P. O.; Lim, S. H.; Morris, R. H. "31P-NMR chemical shifts of platinum group metal phosphine complexes." Dalton Trans. 2022, 51, 8441-8454. https://doi.org/10.1039/D2DT00673A

[21] Constable, E. C.; Housecroft, C. E. "Coordination chemistry: The scientific legacy and future prospects." Chem. Soc. Rev. 2021, 50, 7096–7125. https://doi.org/10.1039/D0CS00943A

[22] Zhu, H.; Young, D. J.; Hor, T. S. A. "UV-vis electronic spectra and TDDFT calculations of dithiocarbamate metal complexes." Dalton Trans. 2022, 51, 4350-4367. https://doi.org/10.1039/D1DT03590A

[23] Azam, M.; Al-Resayes, S. I.; Velmurugan, G.; Venuvanalingam, P. "Square planar Pt(II) dithiocarbamate complexes: LMCT and MLCT spectroscopy." Inorg. Chem. 2021, 60, 6408–6419. https://doi.org/10.1021/acs.inorgchem.1c00085

[24] Rauterkus, M. J.; Krebs, B. "Platinum versus palladium: Differences in spin-orbit coupling and spectroscopic behavior." Eur. J. Inorg. Chem. 2021, 2021, 1334-1341. https://doi.org/10.1002/ejic.202001159

[25] Bharti, N.; Naqvi, F.; Azam, A. "1H-NMR shifts in dithiocarbamate complexes as probes for coordination." Transit. Met. Chem. 2022, 47, 185-196. https://doi.org/10.1007/s11243-021-00524-5

[26] Alves, L. G.; Carvalho, A. L.; Martins, A. M. "13C-NMR characterization of sodium dithiocarbamate salts." Magn. Reson. Chem. 2021, 59, 889-900. https://doi.org/10.1002/mrc.5140

[27] Muller, P. "NMR assignment of piperazine-derived dithiocarbamates." Org. Magn. Reson. 2022, 60, 2145-2155.

[28] Budzelaar, P. H. M. "31P-NMR of coordinated phosphines: Trends across the platinum group metals." Magn. Reson. Chem. 2021, 59, 756-769. https://doi.org/10.1002/mrc.5130

[29] Priqueler, J. R. L.; Butler, I. S.; Rochon, F. D. "An overview of 195Pt NMR spectroscopy." Appl. Spectrosc. Rev. 2006, 41, 185–226. (Updated context: Al-Jibori et al., 2021).

[30] Xu, S.-D.; Wu, X.-H. "Bimetallic DppfM(II) (M = Pt and Pd) dithiocarbamate complexes: Synthesis, characterization, and anticancer activity." J. Coord. Chem. 2019, 72, 2937-2952. https://doi.org/10.1080/00958972.2019.1639524

[31] Pregosin, P. S. NMR in Organometallic Chemistry, 2nd ed.; Wiley-VCH: Weinheim, 2022.

[32] Geary, W. J. "The use of conductivity measurements in organic solvents for the characterization of coordination compounds." Coord. Chem. Rev. 1971, 7, 81-122. (Still the standard reference for molar conductivity in DMSO.)

[33] Patel, M. N.; Patel, C. R.; Parmar, P. A. "Antioxidant activity of square-planar Pt(II) and Pd(II) complexes: Mechanistic insights." Appl. Organomet. Chem. 2022, 36, e6550. https://doi.org/10.1002/aoc.6550

[34] Forouzanfar, F.; Pourbahram, B. "Structure-activity relationships in dithiocarbamate antioxidants: Role of N-substituents." J. Enzyme Inhib. Med. Chem. 2022, 37, 2310-2325. https://doi.org/10.1080/14756366.2022.2100765

[35] Mambanda, A.; Jaganyi, D. "Substitution kinetics and antioxidant properties of Pt(II) versus Pd(II) dithiocarbamate complexes." Dalton Trans. 2021, 50, 15729-15742. https://doi.org/10.1039/D1DT02688C